Chemical Engineering Science 186 (2018) 36–43

Contents lists available at ScienceDirect

Chemical Engineering Science

journal homepage: www.elsevier.com/locate/ces

Manipulating the generation of reactive oxygen species through intermittent hypoxic stress for enhanced accumulation of arachidonic acid-rich lipids

Kun Shi [a], Zhen Gao [a], Lu Lin [b], Wei-Jian Wang [a], Xin-Qiao Shi [a], Xiao Yu [a], Ping Song [a], Lu-Jing Ren [a,d], He Huang [b,c,d], Xiao-Jun Ji [a,d,*]

[a] College of Biotechnology and Pharmaceutical Engineering, Nanjing Tech University, No. 30 South Puzhu Road, Nanjing 211816, People's Republic of China
[b] School of Pharmaceutical Sciences, Nanjing Tech University, No. 30 South Puzhu Road, Nanjing 211816, People's Republic of China
[c] State Key Laboratory of Materials-Oriented Chemical Engineering, Nanjing Tech University, No. 5 Xinmofan Road, Nanjing 210009, People's Republic of China
[d] Jiangsu National Synergetic Innovation Center for Advanced Materials (SICAM), Nanjing Tech University, No. 5 Xinmofan Road, Nanjing 210009, People's Republic of China

HIGHLIGHTS

- Intermittent hypoxia stress reduced ROS generation in *M. alpina*.
- ARA yield increased by about 20% along with a 21% decrease of ROS concentration.
- Biomass, lipid- and ARA concentration simultaneously reached their peak values at the end-point.
- Efficient ARA-rich lipids fermentation was fulfilled by using this strategy.
- The total stirring power of the fermentation was reduced by about 4% in a bioreactor.

GRAPHICAL ABSTRACT

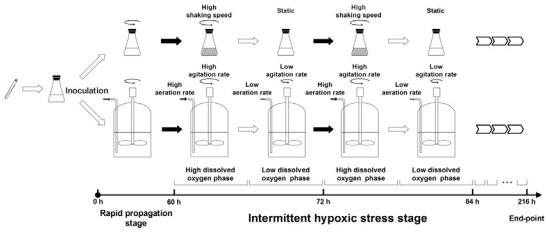

Advantages:

(1) Arachidonic acid production was increased.

(2) Lipid production was increased.

(3) The total stirring power was reduced in a bioreactor.

ARTICLE INFO

Article history:
Received 9 January 2018
Received in revised form 12 April 2018
Accepted 13 April 2018
Available online 13 April 2018

Keywords:
Reactive oxygen species
Arachidonic acid
Intermittent hypoxic stress
Mortierella alpina
Lipid accumulation

ABSTRACT

The accumulation of reactive oxygen species (ROS) can induce oxidative damage which can be detrimental to microbial biomass and product yields. In this study, we used intermittent hypoxic stress (IHS) to eliminate the main source of ROS during the production of arachidonic acid (ARA)-rich lipids by *Mortierella alpina*. Biomass, lipid- and ARA concentration simultaneously reached their peak values, and the ARA yield increased by about 20% along with a lower level of ROS concentration. Under these conditions, more NADPH, substrate and energy may be available for lipid biosynthesis. The efficacy of this strategy was also confirmed in a bioreactor, with similar results. Interestingly, the total power required for stirring fell by about 4%, which may be of practical value for energy savings. This work offers new insights into the control of ROS generation in *M. alpina* and might be applicable to other microbial PUFAs producers.

1. Introduction

As essential components of the cells of higher eukaryotes, polyunsaturated fatty acids (PUFAs) confer flexibility, fluidity and selective permeability properties to membranes, and are indispensable for human health (Ratledge, 2004; Ryan et al., 2010;

* Corresponding author at: College of Biotechnology and Pharmaceutical Engineering, Nanjing Tech University, No. 30 South Puzhu Road, Nanjing 211816, People's Republic of China.
E-mail address: xiaojunji@njtech.edu.cn (X.-J. Ji).

https://doi.org/10.1016/j.ces.2018.04.023
0009-2509/

Ji et al., 2015). Arachidonic acid (ARA) (5, 8, 11, 14-*cis*-eicosatetraenoic acid) is one of the omega-6 PUFAs, and acts as a precursor for the synthesis of eicosanoid hormones such as prostaglandins, leukotrienes and thromboxanes, some of which play an irreplaceable role in combating or preventing a number of human diseases (Dyal and Narine, 2005). The filamentous fungus *Mortierella alpina* is considered the most prominent producer of ARA-rich lipids due to its safety and relatively high production (Higashiyama et al., 2002; Ji et al., 2014).

High dissolved oxygen (DO) is considered a key factor in the ARA biosynthesis process, as PUFAs are formed via an enzymatic desaturation mechanism which requires dioxygen (Nie et al., 2014b). In shake-flask cultures, the level of DO is controlled by changing the shaking speed. However, *M. alpina* is physically weak and sensitive to shear forces, due to which the agitation rate has to be controlled within a precise range (Ji et al., 2014). Furthermore, high DO is not always beneficial for lipid accumulation, and oxygen uptake is not rate-limiting at high oxygen concentrations. It has been reported that filamentous mycelia could not maintain their usual metabolic activity, and had to β-oxidize fatty acids to obtain more energy in order to adapt to high oxygen concentrations (Higashiyama et al., 1999). In addition, it is well established that reactive oxygen species (ROS), which are mainly generated by the electron transfer chain (ETC) in mitochondria, can cause oxidative damage to DNA, proteins, lipids, and other biomolecules (Starkov, 2008; Shi et al., 2017). Our previous research showed that ROS generation significantly increased and antioxidant defenses decreased during the end of fermentation, i.e. during the microbial aging process. Using transmission electron microscopy (TEM), we observed mitochondria that seemed to be enlarged and less compact than normal, which suggested instability, which in turn can cause ROS generation (Yu et al., 2016). Increased oxidative stress may lead to the consumption of stored lipids as energy source in order to maintain cellular homeostasis (Shi et al., 2017). Furthermore, PUFAs can be oxidized by ROS, which may cause unstable ARA production (Yu et al., 2016). In agreement with this, it has been reported in recent years that the external addition of antioxidants, such as sesamol, ginsenosides and ascorbic acid, can scavenge intracellular ROS and improve cell growth and lipid production in oleaginous microorganisms (Ren et al., 2017; Liu et al., 2015). Accordingly, different concentrations of ascorbic acid were supplemented to the fermentation medium in our preliminary experiments. However, no significant changes were found in ARA production, and we even observed a small decline (Table S1). As ME activity and G6PD activity were decline with the addition of ascorbic acid, the lack of NADPH supply may cause the unexpected results (Fig. S1).

In adaptive laboratory evolution, a recovery treatment performed after stimulation may help to ameliorate the increased toxicity due to environmental stresses (Reyes et al., 2014). In this work, we developed a similar strategy to eliminate ROS from the main source—the ETC. This strategy was applied repeatedly in a 12 h cycle after 60 h of fermentation. Each cycle was divided into two phases: a high-DO phase and a low-DO phase for intermittent hypoxic stress (IHS). Considering a predictable delay of cell growth, the agitation speed during the high-DO phase was set at 150 rpm (rpm), which was somewhat higher than the 125 rpm of the original culture. The ARA yield was improved by 20% or more, along with a 21% reduction of intracellular accumulated ROS. Various biochemical parameters like malonic dialdehyde (MDA), glutathione (GSH) and the activities of several key enzymes were evaluated to examine the responses of *M. alpina* to IHS. In addition, the efficacy of this strategy was also tested in a bioreactor and we reached similar results. Interestingly, the total power required for stirring was reduced by about 4%, which may be of practical value for energy savings. This study thus provides a new method for increasing ARA production by removing ROS in *M. alpina*, which also might be used in other microbial PUFA producers.

2. Materials and methods

2.1. Microorganism, media, and culture conditions

M. alpina R807 (CCTCC M2012118), preserved in the China Centre for Type Culture Collection, was used in this study. It was maintained on potato-dextrose agar (PDA) slants at 4 °C, and transferred every 3 months. The PDA medium contained ($g{\cdot}L^{-1}$): potatoes 200, glucose 25, agar 20. The seed culture medium contained ($g{\cdot}L^{-1}$): glucose 30, yeast extract 6, $NaNO_3$ 3, KH_2PO_4 3, $MgSO_4{\cdot}7H_2O$ 0.5. The fermentation medium contained ($g{\cdot}L^{-1}$): glucose 80, yeast extract 10, KH_2PO_4 4, $NaNO_3$ 3, and $MgSO_4{\cdot}7H_2O$ 1.

The culture conditions for *M. alpina* were the same as reported in our previous work (Zhang et al., 2015; Nie et al., 2014a; Peng et al., 2010). Briefly, a sterile loop was used to transfer a small amount of *M. alpina* mycelium from a PDA slant to fresh medium, followed by incubation in an electro-thermal incubator at 25 °C. After 5–7 days of incubation, the resulting mycelia were harvested for seed culture. 500-mL baffled flasks containing 100 mL of appropriate fresh media were used for seed culture and fermentation culture. Seed culture was conducted for 18–24 h at 25 °C, after which the resulting culture was used to inoculate the fermentation broth at 10% (v/v). After a course of regular fermentation, mycelia were continuously cultured without carbon source to initiate the aging process (Zhang et al., 2015). Shake-flask cultivation was carried out at 25 °C and 125 rpm, with an initial pH of 6.0. ARA batch fermentation was carried out in a 1-L bioreactor (Solaris Biotechnology, Italy) containing 0.6 L of fermentation medium, using a previously reported multi-stage fermentation strategy (Wu et al., 2017).

The procedures of the new IHS strategy are shown in Graphical abstract. This strategy was conducted repeatedly in a 12 h cycle after 60 h of fermentation. Each cycle was divided into two phases: a high-DO phase, and a low-DO phase for periodic hypoxia treatment. The DO of the high-DO phase was slightly above normal.

2.2. Analysis of glucose concentration, dry cell weight, total lipids, and fatty acid profiles

Glucose concentrations were analyzed using an SBA-40C glucose oxidase electrode (Biology Institute of Shandong Academy of Sciences, China). The biomass density was measured by determining the DCW of mycelia that were harvested and separated by filtration through a conventional filter paper, washed three times, and dried at 50 °C to constant weight (approx. 24 h). The analysis of total lipids and the fatty acid profiles was carried out according to our previously reported methods (Zhang et al., 2015). Polynomial fittings of the 4th order was used to describe the kinetics of DCW, lipid/DCW and ARA/total fatty acids (TFAs), using Origin 8.0 (Microcal Software Inc., Northampton, MA, USA).

2.3. Measurement of intracellular ROS

The contents of ROS in *M. alpina* mycelia was determined according to our previously reported methods (Yu et al., 2016). Briefly, the mycelia were harvested and incubated with 10 $\mu g\ mL^{-1}$ of DCFH-DA (Dichloro-dihydro-fluorescein diacetate, prepared in DMSO; Sigma-Aldrich, MO, USA) with shaking at 25 °C for 30 min, washed three times by centrifuging at 8000*g* for 10 min and resuspending in phosphate buffer solution (PBS, pH 7.4). The fluorescence density (FLU) was recorded using a SpectraMax M3 fluorescence spectrophotometer (Molecular Devices, CA, USA)

using excitation and emission wavelengths of 488 nm and 525 nm, respectively. The relative fluorescence density (RFLU) was calculated by dividing the FLU by the DCW.

2.4. Enzyme activity assays, determination of MDA and GSH

Preparation of cell extracts was carried out according to our previously reported methods (Sun et al., 2016). Protein concentrations were determined using the Bradford method with bovine serum albumin (BSA) as the standard. Total protein content of the crude enzyme preparations was calculated using an empirically determined calibration equation. The cell extracts were recovered for the determination of MDA, GSH, malic enzyme (ME), glucose-6-phosphate dehydrogenase (G6PD), catalase (CAT), ATP:citrate lyase (ACL), and isocitrate dehydrogenase (ICD) activities using commercially available assay kits (AngleGene, Nanjing, China), according to the manufacturer's instructions. Normal saline was negative control in enzyme activity assays.

2.5. Confocal fluorescence microscopy

Confocal fluorescence microscopy was conducted according to our previously reported methods (Yu et al., 2017). The mycelia were collected by centrifugation and resuspended in PBS buffer (pH 7.4) to a final concentration of 0.1 g/mL. An aliquot comprising 5 μL of Nile Red stock solution (0.4 mg/mL; J & K Scientific Ltd, China) was added to 3 mL of the mycelia-in-PBS suspension and shaken gently for 1 min. After incubation in darkness for 5–10 min at room temperature, samples were directly used for microscopic analysis (FV1000, Olympus, Japan). The fluorescence excitation wavelength was set at 488 nm and the emission wavelength scanning range was set from 500 nm to 750 nm.

2.6. Statistical analysis

The mean values and the standard error of the mean were calculated from the data obtained from three biological replicates. A statistical analysis of the obtained data was carried out using Origin 8.0 software (Microcal Software Inc., Northampton, MA, USA). One way analysis of variance (ANOVA) with *t*-test was conducted on the data, and $P < 0.05$ was considered significantly different.

3. Results and discussion

3.1. Changes of cell growth, substrate consumption, lipid- and ARA accumulation under IHS

In shake-flask cultures, the DO level can be controlled by changing the shaking speed, since more vigorous agitation can force more oxygen into the fermentation broth (Higashiyama et al., 1999). We therefore chose static culture to induce low-oxygen conditions in this study. As shown in Table 1, *M. alpina* was cultured in shake flasks that were kept static for different periods of time. The results indicated that the optimum conditions of IHS were static culture for 1 h every 12 h, which lead to simultaneous increases of DCW, total lipids and ARA yield. Perhaps unsurprisingly, too long periods of low oxygen actually decreased the accumulation of ARA-rich lipids and inhibited cell growth. Our solution to this problem was to increase the shaking speed during the high-DO phases. As shown in Table 1, the optimum shaking speed appeared to be 150 rpm, which led to the highest ARA yield of 6.56 g/L, and was consequently chosen for the IHS in further experiments.

As shown in Fig. 1A and B, IHS caused significant changes in the substrate consumption and growth profiles of *M. alpina*. Although we increased the shaking speed from 125 rpm to 150 rpm, IHS still reduced the consumption of glucose, and prolonged the time until substrate depletion by about 2 days. Similarly, IHS resulted in a decrease of the cell growth rate, and postponed the time of the DCW peak from 144 h to 192 h. Interestingly, these results were not in line with previous studies, in which continuous low oxygen was found to have no considerable effect on the time course of DCW in *M. alpina* (Higashiyama et al., 1999; Dedyukhina et al., 2015).

The aging technology developed recently for *M. alpina*, which cultures the cells for several days without carbon source after regular fermentation, can significantly increase the ARA content in the TFAs (Bajpai et al., 1991). However, biomass and lipid production decreased significantly during the aging process (Jin et al., 2009; Zhang et al., 2015). As shown in Fig. 1A and C, the DCW and lipid concentration of the control increased to 28.07 and 13.17 g/L at the end of regular fermentation, but decreased to 24.49 and 10.69 g/L during the aging process, respectively. Since IHS may prolong the fermentation period and shorten the aging process, the loss of biomass and lipid production could be decreased greatly. The DCW of the IHS group reached 28.03 g/L at 216 h, which was about 15% higher than that of the control. Moreover, a significant improvement of lipid concentration was achieved under IHS, with an increase of 30.9% over that of the control.

Lipids are usually stored in lipid droplets (LDs) after being synthesized in the endoplasmic reticulum (Ji et al., 2014). To further investigate how the morphology of LDs changed under IHS, confocal microscopy was employed. As depicted in Fig. 2, at the end of fermentation under IHS (216 h), a large proportion of the cell volume was occupied by LDs, and both the number and the size of LDs increased significantly compared to the control. Moreover, the variation of LDs was in accordance with the trend of lipid/DCW shown in Fig. 1D, which increased by 14.3% compared with the control.

ARA is formed through elongation and desaturation, in a complex set of reactions starting from a suitable carbon source in the

Table 1
Comparison of the effects of different intermittent hypoxic stress regimens on dry cell weight, lipid- and arachidonic acid yield at 216 h. Values are presented as the mean ± standard deviation (n = 3). Values with the different letters represent a significant difference ($P < 0.05$) between treatments. (DCW: dry cell weight, ARA: arachidonic acid, rpm: revolutions per minute).

A cycle		Shaking speed (rpm)	DCW (g/L)	Lipid (g/L)	ARA (g/L)
Static time (h)	Shaking time (h)				
0	12	125	24.49 ± 0.02^{b}	10.69 ± 0.55^{ab}	5.48 ± 0.01^{bc}
0.5	11.5	125	24.97 ± 0.21^{c}	11.49 ± 0.51^{b}	5.84 ± 0.07^{c}
1	11	125	25.04 ± 0.19^{c}	12.05 ± 0.36^{b}	6.02 ± 0.03^{d}
2	10	125	26.05 ± 0.15^{d}	13.89 ± 0.21^{c}	5.02 ± 0.27^{b}
1	11	135	26.19 ± 0.07^{d}	12.79 ± 0.22^{bc}	6.27 ± 0.06^{d}
1	11	150	28.03 ± 0.08^{e}	13.99 ± 0.10^{c}	6.56 ± 0.06^{e}
1	11	175	28.18 ± 0.07^{e}	12.32 ± 0.11^{b}	5.59 ± 0.13^{bc}
1	11	200	24.16 ± 0.03^{a}	9.76 ± 0.20^{a}	3.94 ± 0.09^{a}

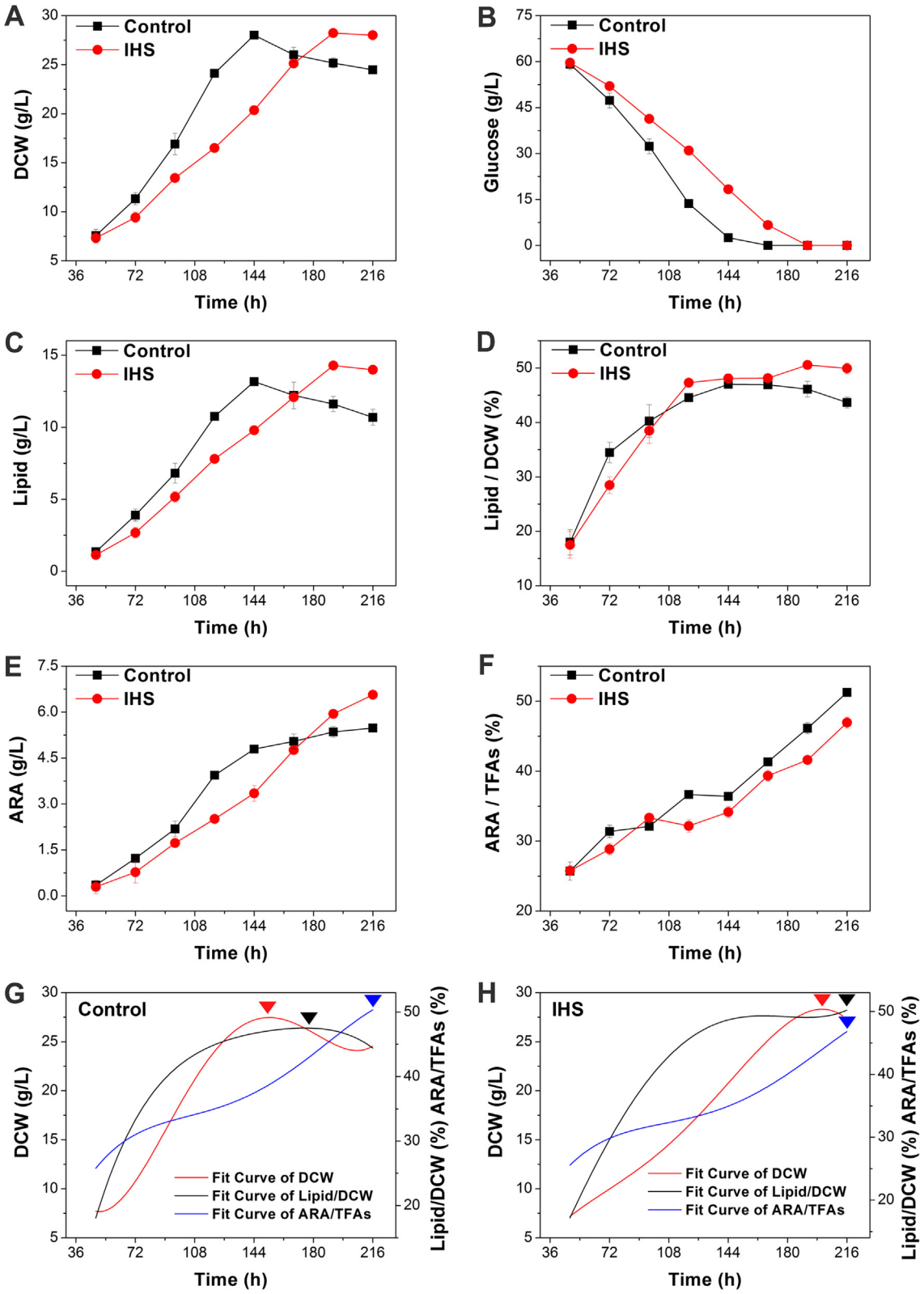

Fig. 1. Time course of dry cell weight (DCW) (A), glucose concentration (B), lipid yield (C), lipid/DCW (D), arachidonic acid (ARA) yield (E), ARA/total fatty acids (TFAs) (F) and fitting values of DCW, lipid/DCW and ARA/TFAs. Values are presented as the mean ± standard deviation (n = 3). (The control group is marked with a G and the intermittent hypoxic stress (IHS) group with an H).

mycelia. The desaturation involves an aerobic oxygenation reaction, and DO is thus considered to be a key factor in ARA biosynthesis (Higashiyama et al., 1999; Nie et al., 2014b). Accordingly, several studies showed the negative effect of oxygen limitation on ARA accumulation in *M. alpina* (Higashiyama et al., 2002; Wu et al., 2017; Zhang et al., 2017). As shown in Fig. 1F and Table 2,

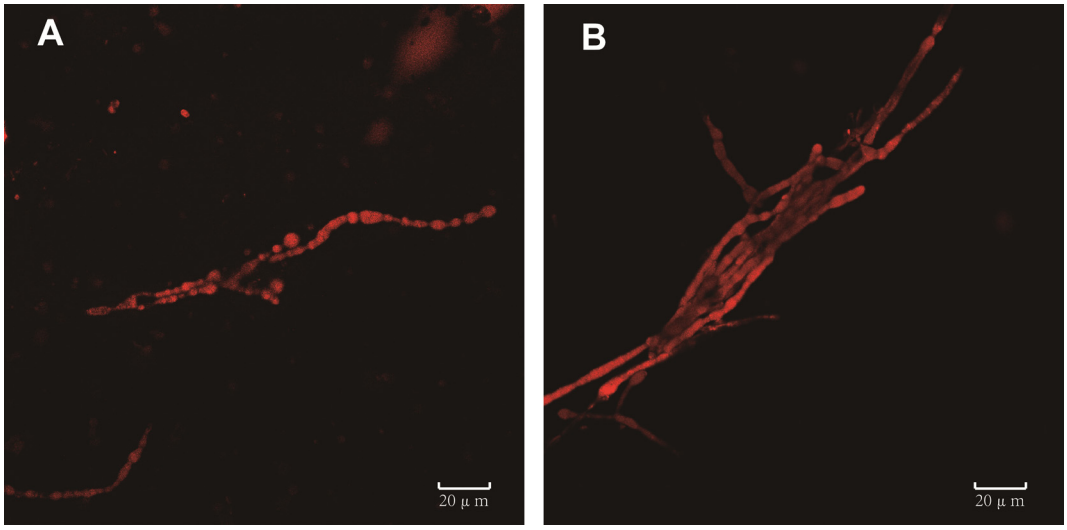

Fig. 2. Fluorescence microscopic images of mycelia at 216 h of culture. (The control group marked with an A and the intermittent hypoxic stress group with a B).

Table 2
Changes of the percentage of arachidonic acid (C20:4) and various other fatty acids in total fatty acids under intermittent hypoxic stress (IHS). Values are presented as the mean ± standard deviation (n = 3). The statistical significance between control group and IHS group was presented by *t*-test, respectively. (*, $p < 0.05$).

Fatty acids	Control (%)	IHS (%)	Increase
C16:0	8.92 ± 0.07	11.56 ± 0.62*	29.60%
C18:0	13.58 ± 0.08	14.02 ± 0.11	3.24%
C18:1	15.05 ± 0.21	14.63 ± 0.37	−2.79%
C18:2	5.98 ± 0.23	6.92 ± 0.49*	15.72%
C18:3	3.58 ± 0.05	3.27 ± 0.02*	−8.66%
C20:4	51.26 ± 0.39	46.94 ± 0.80*	−8.43%
Others	2.63 ± 0.03	2.65 ± 0.07	0.76%

our results were in line with previous work. The ARA/TFAs was 46.96% under IHS, which was lower than the 51.26% in the control. Nevertheless, as ARA is an intracellular liposoluble product, the achievement of a higher biomass density and lipid accumulation is essential for ARA production. Owing to this, the ARA yield reached 6.56 g/L at 216 h, which was about 20% higher than that of the control (Fig. 1E). The data in Table 2 indicate that the percentages of C16:0 and C18:2 increased, while those of ARA and C18:3 decreased synchronously. The linoleic acid (LA, C18:2, omega-6) is transformed to γ-linolenic acid (GLA, C18:3, omega-6) by delta 6-desaturase (EC 1.14.99.-) (Ji et al., 2014). Our result indicates that the key enzyme controlled by DO in ARA biosynthesis may be delta 6-desaturase.

In our previous work, it was found that an optimal fermentation process for the production of ARA-rich lipids incorporates three stages— mycelial propagation, lipid biosynthesis, and ARA accumulation (Nie et al., 2014a). As shown in Fig. 1G and H, kinetic studies were performed to conduct a comparative analysis of the effects of IHS on product formation. The biomass, lipid- and ARA concentration of the control group reached their respective maximum values at 153 h, 175 h and 216 h (arrows with different colors in Fig. 1G). Most fermentation strategies optimized only one indicator, such as media with carbon limitation, which promote the rapid accumulation of ARA but are not beneficial for mycelial growth and lipid accumulation (Bajpai et al., 1991; Jin et al., 2009). In practical industrial production, the final ARA-rich lipid is usually diluted to a standardized level of 40% ARA/TFAs by adding vegetable oil, which indicates that excessively high ARA concentrations may be not required (Ji et al., 2014). Similarly, nitrogen limitation is a requisite for lipid biosynthesis but may result in decreased biomass and consequently decreased total ARA yields (Nie et al., 2014a). Hence, it is more effective to find a balance between DCW, lipid/DCW and ARA/TFAs to reach the highest possible total ARA yield. As shown in Fig. 1H, all three production peaks occurred at the end of fermentation under IHS. This is possible due to a balancing of the different oxygen requirements of cell growth (including DNA replication and protein synthesis), lipid accumulation and ARA biosynthesis.

3.2. Changes of activities of key enzymes involved in lipid biosynthesis under IHS

In order to investigate whether the increase of lipid accumulation under IHS was related to a shift of metabolic pathways, the activities of four key enzymes in the lipid biosynthesis pathway were measured every 2 days after 120 h of fermentation (Fig. 3).

NADPH is known to be a key cofactor required for fatty acid synthesis and desaturation in *M. alpina*, and it can be generated by several enzymes, such as malic enzyme (ME), glucose-6-phosphate dehydrogenase (G6PD) and isocitrate dehydrogenase (ICD) (Ji et al., 2014). Hao et al. (2016) found that G6PD had the most significant effect on fatty acid synthesis, whereas ME was more effective for increasing desaturation in *M. alpina*. Yu et al. (2016) found that ICD might provide additional NADPH for ARA synthesis during the aging process. As shown in Fig. 3A, B and C, those activities of all three key enzymes increased under IHS, which may imply that more NADPH was produced. These results were in good agreement with the observed changes of fermentation characteristics and LD morphology.

ICD is a key enzyme in the TCA cycle and plays a crucial role in the energy metabolism (Hao et al., 2016; Wynn & Ratledge, 2005). As shown in Fig. 3C, strains under IHS exhibited an overall increase of ICD activity compared with the control, with 516 U/mg protein at 120 h—a 263% increase. This increased TCA activity may provide more ATP for cell growth, which might explain the higher DCW in the IHS group at the end of fermentation (Fig. 1A). In the cytosol, ACL cleaves citrate into oxaloacetate and acetyl-CoA, which is further converted to malonyl-CoA by ACC for the synthesis of fatty acids, including ARA (Ji et al., 2014). Accordingly, a higher level of ACL activity was observed under IHS. Especially during the lipid accumulation stage (120 h), ACL activity showed a peak value of 667 U/mg protein, which corresponds to a 37% increase over the

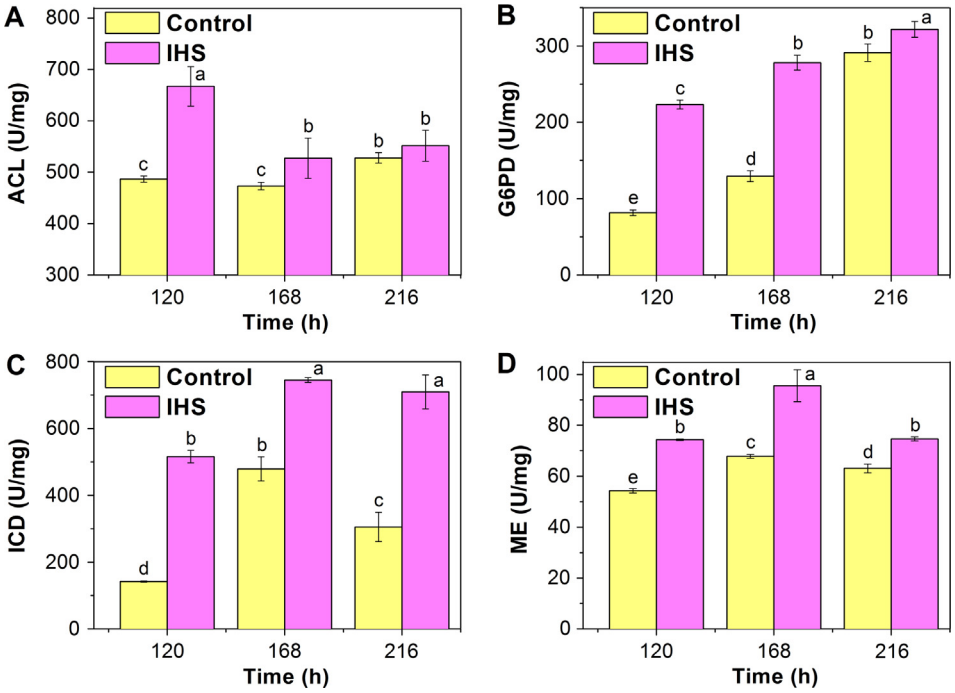

Fig. 3. Changes of activities of key enzymes involved in lipid biosynthesis under intermittent hypoxic stress (IHS). ATP citrate lyase (ACL) (A), glucose-6-phosphate dehydrogenase (G6PD) (B), isocitrate dehydrogenase (ICD) (C), and malic enzyme (ME) (D). Values are presented as the mean ± standard deviation (n = 3). Values with the different letters represent a significant difference ($P < 0.05$) between treatments.

control (Fig. 3A). These results indicate that carbohydrate metabolic pathways may be up-regulated under IHS, leading to increased substrate and energy supply for lipid accumulation.

3.3. Changes of ROS and antioxidative defense systems under IHS

Reactive oxygen species (ROS), such as superoxide (O_2^-), hydroxyl radical (OH•), and hydrogen peroxide (H_2O_2), are formed by the partial reduction of oxygen, which is an inevitable aspect of life under aerobic conditions (Caspeta et al., 2014; Montibus et al., 2015; Shi et al., 2017). The accompanying ROS-induced oxidative stress may reduce cell viability and deactivate critical enzymes, ultimately resulting in cellular toxicity (Chokshi et al., 2015). Moreover, PUFAs such as ARA are highly susceptible to attack by oxygen radicals, and oxidative stress may therefore directly limit lipid productivity (Xu et al., 2017). Furthermore, high levels of ROS may lead to the consumption of stored lipids as an energy source in order to maintain cellular homeostasis. Several efforts such as the external addition of antioxidants and upregulation of oxidative stress defense pathways can be used to scavenge intracellular ROS in order to improve cell growth and lipid production in oleaginous microorganisms (Ren et al., 2017; Liu et al., 2015; Xu et al., 2017).

Considering that the mitochondrial electron transport chain is a major source of ROS, we speculated that oxygen limitation may help reduce ROS generation (Shi et al., 2017). The time profiles of ROS levels during cultivation shown in Fig. 4A, confirmed our hypothesis. During the aging process, the amount of ROS significantly increased in the control but remained relatively low under IHS.

Lipid peroxidation is the process in which ROS attack PUFAs of the cellular membrane, leading to chain reactions that result in membrane damage (Melegari et al., 2012). Malondialdehyde (MDA) is a natural biomarker produced during lipid peroxidation which can be used as an indicator of the cell damage produced by ROS (Chokshi et al., 2015). As shown in Fig. 4B, MDA content was lower under IHS than in the control, corresponding to the ROS content at the end of the culture. It is likely that IHS minimizes the loss of biomass and lipids during the aging process, which might be the key reason for the high DCW and increased lipid accumulation.

The cellular ROS metabolism is tightly regulated by a battery of biological redox balance mechanisms, including both antioxidant enzymes (e.g. CAT) and non-enzymatic metabolites (e.g. GSH) (Shi et al., 2017). In the present study, both the levels of CAT and GSH decreased under IHS, which indicated that they may not be the drivers of the increased performance under IHS, but were instead reduced as a result of lower ROS (Fig. 4C and D). In fact, it is possible that NADPH flux that was released by the reduction of intracellular accumulated ROS was diverted from the antioxidant system towards lipid biosynthesis. This might be another underlying cause of higher lipid production under IHS.

3.4. Batch fermentation in a bioreactor under IHS

In large-scale industrial bioreactors, the level of DO is increased by manipulating the agitation speed, which often leads to unacceptable power consumption (Nie et al., 2014b; Clarke et al., 2006; Guo et al., 2017). We expected that the fermentation process under IHS may reduce the power consumption required for stirring. Small-scale bioreactors enable increases in the rate at which the necessary experiments are performed, thus reducing fermentation development times and costs (Lye et al., 2003; Micheletti and Lye, 2006; Gill et al., 2008). The fermentation under IHS was also carried out in a small-scale bioreactor to identify key parameters and discuss the potential for large-scale production using this strategy.

In our previous work, a multi-stage fermentation strategy based on precise control of DO at proper times was developed in a 7.5-L bioreactor (Wu et al., 2017). In this study, we further combined this multi-stage fermentation strategy with IHS in a fed-batch system. To enable rapid propagation and reduce the shear force, the

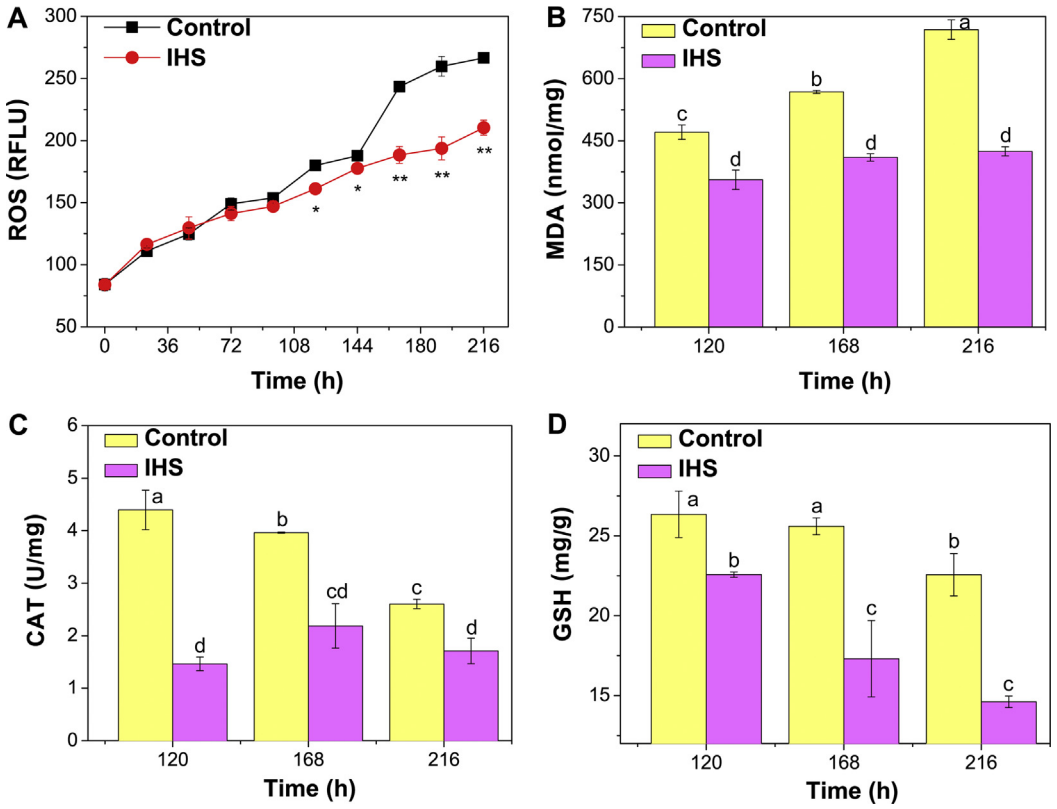

Fig. 4. Changes of catalase (CAT) (A), malonic dialdehyde (MDA) (B), glutathione (GSH) (C), and reactive oxygen species (ROS) (D) under intermittent hypoxic stress (IHS) (relative fluorescence density: RFLU). Values are presented as the mean ± standard deviation (n = 3). Values with the different letters represent a significant difference ($P < 0.05$) between treatments. (*, $p < 0.05$, **, $p < 0.01$).

aeration rate was set at 400 Nml/min, with a lower agitation speed of 50 rpm in Stage I (0–60 h). The agitation speed and aeration rate were increased stepwise from 50 to 160 rpm (150 rpm in control group) and 400 to 550 Nml/min, respectively, with IHS in Stage II (60–120 h). In Stage III (120–216 h), the agitation speed was further increased to 210 rpm with IHS (200 rpm was the speed for the control). As shown in Table 3, we obtained similar results to those of shake-flask cultures. The lipid yield of the IHS group was about 31% higher than that of the control, but a slight reduction of ARA accumulation was observed. The ARA yield reached 6.78 g/L at 216 h, which was about 17% higher than that of the control. Due to the convenience in practical operation and huge market potential, the IHS strategy with 17% increase has a promising future with considerable benefits. As shown in Fig. 5, the new three-stage fermentation strategy with IHS resulted in several periodic reductions of DO, which fitted well with the changes of stirring power. At the low-DO phase of each cycle, the average decline of stirring power reached about 85%. However, as a result of a slight increase of agitation speed at each high-DO phase, the total stirring power of the fermentation only fell by about 4%.

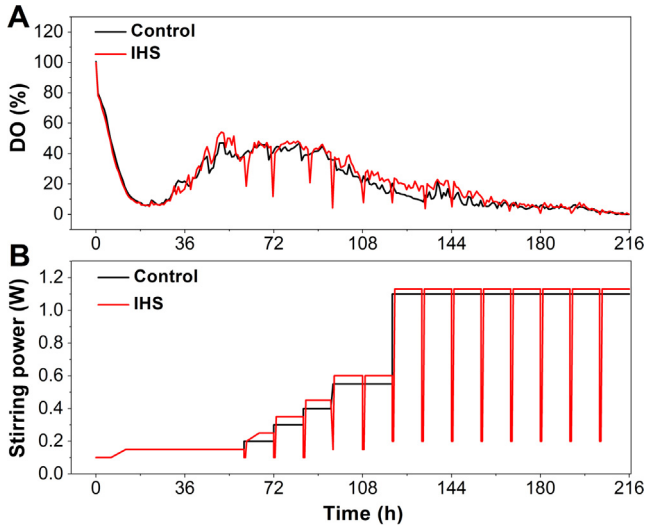

Fig. 5. Time course of dissolved oxygen (DO) (A) and stirring power (B) under intermittent hypoxic stress (IHS) in a bioreactor.

Table 3
Fermentation parameters at 216 h in the bioreactor. Values are presented as the mean ± standard deviation (n = 3). The statistical significance between control group and IHS group was presented by *t*-test, respectively. (DCW: dry cell weight, ARA: arachidonic acid, TFAs: total fatty acids, IHS: intermittent hypoxic stress, *: $p < 0.05$).

Parameters	Control	IHS	Increase (%)
DCW (g/L)	24.16 ± 0.14	25.19 ± 0.43	4.3
Lipid (g/L)	9.76 ± 0.24	12.79 ± 0.17*	31.1
Lipid/DCW (%)	40.40 ± 0.72	50.76 ± 0.33*	25.6
ARA (g/L)	5.80 ± 0.12	6.78 ± 0.09*	16.9
ARA/TFAs (%)	59.39 ± 0.63	53.00 ± 1.02*	−10.8

Nevertheless, given the energy consumption in industrial-scale production, the IHS strategy may amount to significant reductions of total power consumption.

4. Conclusion

In this work, we developed a new strategy to produce ARA-rich lipids by manipulating ROS generation via IHS. The kinetic studies

showed that DCW, lipid- and ARA concentration simultaneously reached their respective peak values at the end of fermentation under IHS. *M. alpina* cultured under IHS in shake-flasks produced a higher DCW, lipid- and ARA yield than the control. These major performance changes were accompanied by a reduction of intracellular accumulated ROS, which likely improved cell viability and reduced the oxidative damage. All the measured enzymatic NADPH sources were upregulated, which was accompanied by a decline of NADPH consumption by antioxidant systems, indicating that more NADPH may have been channeled into lipid biosynthesis under IHS. Carbohydrate metabolic pathways were upregulated, which indicated an increased supply of substrates and energy for lipid accumulation. Finally, this new strategy was also applied to a bioreactor batch culture, and reached similar results. Interestingly, the total stirring power of the fermentation was reduced by about 4%, which may be of practical value for energy savings in industry. This work thus provides an innovative method for increasing ARA production by removing ROS in *M. alpina*, which also might be applicable to other microbial PUFA producers.

Acknowledgments

This work was financially supported by the National Natural Science Foundation of China (Nos. 21776131, 21476111 and 21376002), the Program for Innovative Research Team in University of Jiangsu Province, the Priority Academic Program Development of Jiangsu Higher Education Institutions, the Jiangsu Synergetic Innovation Center for Advanced Bio-Manufacture (No. XTD1814), and Top-notch Academic Programs Project of Jiangsu Higher Education Institutions (No. PPZY2015B155).

Appendix A. Supplementary material

Supplementary data associated with this article can be found, in the online version, at https://doi.org/10.1016/j.ces.2018.04.023.

References

Bajpai, P., Bajpai, P.K., Ward, O.P., 1991. Effects of aging *Mortierella* mycelium on production of arachidonic and eicosapentaenoic acids. J. Am. Oil Chem. Soc. 68 (10), 775–780.

Caspeta, L., Chen, Y., Ghiaci, P., Feizi, A., Buskov, S., Hallstrom, B.M., Nielsen, J., 2014. Biofuels. Altered sterol composition renders yeast thermotolerant. Science 346 (6205), 75–78.

Chokshi, K., Pancha, I., Trivedi, K., George, B., Maurya, R., Ghosh, A., Mishra, S., 2015. Biofuel potential of the newly isolated microalgae Acutodesmus dimorphus under temperature induced oxidative stress conditions. Bioresour. Technol. 180, 162–171.

Clarke, K.G., Williams, P.C., Smit, M.S., Harrison, S.T.L., 2006. Enhancement and repression of the volumetric oxygen transfer coefficient through hydrocarbon addition and its influence on oxygen transfer rate in stirred tank bioreactors. Biochem. Eng. J. 28 (3), 237–242.

Dedyukhina, E.G., Chistyakova, T.I., Mironov, A.A., Kamzolova, S.V., Minkevich, I.G., Vainshtein, M.B., 2015. The effect of pH, aeration, and temperature on arachidonic acid synthesis by *Mortierella alpina*. Appl. Biochem. Microbiol. 51 (2), 242–248.

Dyal, S.D., Narine, S.S., 2005. Implications for the use of *Mortierella* fungi in the industrial production of essential fatty acids. Food Res. Int. 38 (4), 445–467.

Gill, N.K., Appleton, M., Baganz, F., Lye, G.J., 2008. Quantification of power consumption and oxygen transfer characteristics of a stirred miniature bioreactor for predictive fermentation scale-up. Biotechnol. Bioeng. 100 (6), 1144–1155.

Guo, D.S., Ji, X.J., Ren, L.J., Li, G.L., Huang, H., 2017. Improving docosahexaenoic acid production by Schizochytrium sp using a newly designed high-oxygen-supply bioreactor. Aiche J. 63 (10), 4278–4286.

Hao, G., Chen, H., Gu, Z., Zhang, H., Chen, W., Chen, Y.Q., 2016. Metabolic engineering of *Mortierella alpina* for enhanced arachidonic acid production through the NADPH-supplying strategy. Appl. Environ. Microbiol. 82 (11), 3280–3288.

Higashiyama, K., Fujikawa, S., Park, E.Y., Shimizu, S., 2002. Production of arachidonic acid by*Mortierella* fungi. Biotechnol. Bioprocess Eng. 7 (5), 252–262.

Higashiyama, K., Murakami, K., Tsujimura, H., Matsumoto, N., Fujikawa, S., 1999. Effects of dissolved oxygen on the morphology of an arachidonic acid production by *Mortierella alpina* 1S–4. Biotechnol. Bioeng. 63 (4), 442–448.

Ji, X.J., Ren, L.J., Huang, H., 2015. Omega-3 biotechnology: a green and sustainable process for Omega-3 fatty acids production. Front. Bioeng. Biotechnol. 3, 158.

Ji, X.J., Ren, L.J., Nie, Z.K., Huang, H., Ouyang, P.K., 2014. Fungal arachidonic acid-rich oil: research, development and industrialization. Crit. Rev. Biotechnol. 34 (3), 197–214.

Jin, M.J., Huang, H., Xiao, A.H., Gao, Z., Liu, X., Peng, C., 2009. Enhancing arachidonic acid production by *Mortierella alpina* ME-1 using improved mycelium aging technology. Bioprocess Biosyst. Eng. 32 (1), 117–122.

Liu, B., Liu, J., Sun, P., Ma, X., Jiang, Y., Chen, F., 2015. Sesamol enhances cell growth and the biosynthesis and accumulation of docosahexaenoic acid in the Microalga *Crypthecodinium cohnii*. J. Agric. Food Chem. 63 (23), 5640–5645.

Lye, G.J., Ayazishamlou, P., Baganz, F., Dalby, P.A., Woodley, J.M., 2003. Accelerated design of bioconversion processes using automated microscale processing techniques. Trends Biotechnol 21 (1), 29–37.

Melegari, S.P., Perreault, F., Moukha, S., Popovic, R., Creppy, E.E., Matias, W.G., 2012. Induction to oxidative stress by saxitoxin investigated through lipid peroxidation in Neuro 2A cells and *Chlamydomonas reinhardtii* alga. Chemosphere 89 (1), 38–43.

Micheletti, M., Lye, G.J., 2006. Microscale bioprocess optimisation. Curr. Opin. Biotechnol. 17 (6), 611–618.

Montibus, M., Pinson-Gadais, L., Richard-Forget, F., Barreau, C., Ponts, N., 2015. Coupling of transcriptional response to oxidative stress and secondary metabolism regulation in filamentous fungi. Crit. Rev. Microbiol. 41 (3), 295–308.

Nie, Z.K., Deng, Z.T., Zhang, A.H., Ji, X.J., Huang, H., 2014a. Efficient arachidonic acid-rich oil production by *Mortierella alpina* through a three-stage fermentation strategy. Bioprocess Biosyst. Eng. 37 (3), 505–511.

Nie, Z.K., Ji, X.J., Shang, J.S., Zhang, A.H., Ren, L.J., Huang, H., 2014b. Arachidonic acid-rich oil production by *Mortierella alpina* with different gas distributors. Bioprocess Biosyst. Eng. 37 (6), 1127–1132.

Peng, C., Huang, H., Ji, X.J., Liu, X., Ren, L.J., Yu, W.T., Lu, J.M., 2010. Effects of n-hexadecane concentration and a two-stage oxygen supply control strategy on arachidonic acid production by *Mortierella alpina* ME-1. Chem. Eng. Technol. 33 (4), 692–697.

Ratledge, C., 2004. Fatty acid biosynthesis in microorganisms being used for single cell oil production. Biochimie 86 (11), 807–815.

Ren, L.J., Sun, X.M., Ji, X.J., Chen, S.L., Guo, D.S., Huang, H., 2017. Enhancement of docosahexaenoic acid synthesis by manipulation of antioxidant capacity and prevention of oxidative damage in Schizochytrium sp. Bioresour. Technol. 223, 141–148.

Reyes, L.H., Gomez, J.M., Kao, K.C., 2014. Improving carotenoids production in yeast via adaptive laboratory evolution. Metab. Eng. 21, 26–33.

Ryan, A. S., Zeller, S., Nelson, E. B., Cohen, Z., Ratledge, C. (2010). Safety evaluation of single cell oils and the regulatory requirements for use as food ingredients. In Cohen Z., Ratledge C., (Eds.), Single Cell Oils. Microbial and Algal Oil, second ed. (pp. 317–350).

Shi, K., Gao, Z., Shi, T.Q., Song, P., Ren, L.J., Huang, H., Ji, X.J., 2017. Reactive oxygen species-mediated cellular stress response and lipid accumulation in oleaginous microorganisms: the state of the art and future perspectives. Front. Microbiol. 8, 793.

Starkov, A.A., 2008. The role of mitochondria in reactive oxygen species metabolism and signaling. Ann. NY Acad. Sci. 1147 (1), 37–52.

Sun, X.M., Ren, L.J., Ji, X.J., Chen, S.L., Guo, D.S., Huang, H., 2016. Adaptive evolution of *Schizochytrium* sp. by continuous high oxygen stimulations to enhance docosahexaenoic acid synthesis. Bioresour. Technol. 211, 374–381.

Wu, W.J., Zhang, A.H., Peng, C., Ren, L.J., Song, P., Yu, Y.D., Ji, X.J., 2017. An efficient multi-stage fermentation strategy for the production of microbial oil rich in arachidonic acid in *Mortierella alpina*. Bioresour. Bioprocess. 4 (1), 8.

Wynn, J. P., Ratledge, C. (2005). Oils from Microorganisms. In Shahidi F., (Ed.), Bailey's Industrial Oil and Fat Products. John Wiley & Sons, Inc.

Xu, P., Qiao, K., Stephanopoulos, G., 2017. Engineering oxidative stress defense pathways to build a robust lipid production platform in Yarrowia lipolytica. Biotechnol. Bioeng. 114 (7), 1521–1530.

Yu, Y., Li, T., Wu, N., Jiang, L., Ji, X., Huang, H., 2017. The role of lipid droplets in *Mortierella alpina* aging revealed by integrative subcellular and whole-cell proteome analysis. Sci. Rep. 7, 43896.

Yu, Y., Li, T., Wu, N., Ren, L., Jiang, L., Ji, X., Huang, H., 2016. Mechanism of arachidonic acid accumulation during aging in *Mortierella alpina*: a large-scale label-free comparative proteomics study. J. Agric. Food Chem. 64 (47), 9124–9134.

Zhang, A.H., Ji, X.J., Wu, W.J., Ren, L.J., Yu, Y.D., Huang, H., 2015. Lipid fraction and intracellular metabolite analysis reveal the mechanism of arachidonic acid-rich oil accumulation in the aging process of *Mortierella alpina*. J. Agric. Food Chem. 63 (44), 9812–9819.

Zhang, X., Jiang, L., Zhu, L.Y., Shen, Q.K., Ji, X.J., Huang, H., Zhang, H.M., 2017. Effects of aeration on metabolic profiles of *Mortierella alpina* during the production of arachidonic acid. J. Ind. Microbiol. Biotechnol. 44 (8), 1225–1235.